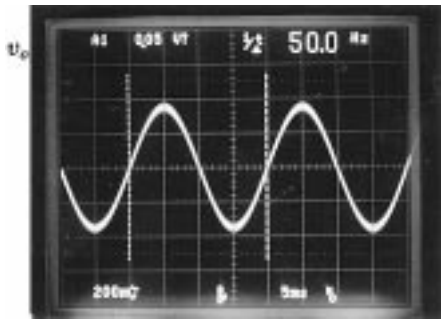

Fig. 5. Output voltage waveform in the closed-loop dc-ac power inverter. Horizontal scale: 5 ms/div.; vertical scale: 0.2 V/div.

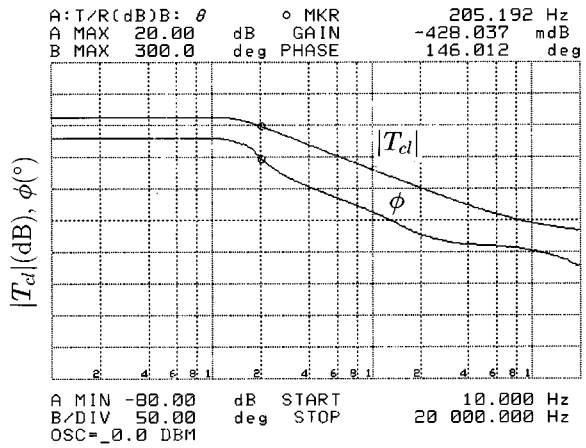

Fig. 6. Bode plots of the closed-loop power inverter $\boldsymbol{T}_{\mathrm{cl}}$.

Packard 4194A Network Analyzer, Bode plots were measured for the closed-loop system. The results are depicted in Fig. 6. It can be seen that the –3-dB frequency was 205 Hz.

IV. Conclusion

This study demonstrates that a low-frequency dc-ac power inverter constructed from a Σ-Δ modulator and a half-bridge inverter is capable of reproducing a very high-quality sine wave. Although this technique was demonstrated using low-power devices, a high-power circuit would behave identically. However, a design of such an inverter is currently impaired by the fact that the switching frequency varies by an, as of yet, unpredictable way. This potentially weak point requires more research.

The most obvious application of this technique is inversion to operate ac devices from dc sources, such as cars or recreational vehicles, or in uninterruptible power supplies and motor drives. Additionally, this circuit could easily be extended to provide amplification for self-powered subwoofers. dc-dc conversion is also possible.

Further work should include a digital implementation of a Σ-Δ modulator control circuit and an increased system bandwidth. A digital implementation would allow direct digital-to-high-power applications, such as programmable inverters with variable frequency and variable amplitude or three-phase regulation. Increasing the bandwidth of the system would allow the technique to be used for audio amplification. Fair comparison of the performance of this technique and other control schemes requires more research. In addition, characterization of behavior with nonlinear loads is recommended for further research.

References

[1] N. Mohan, T. M. Undeland, and W. P. Robbins, *Power Electronics*, 2nd ed. New York, NY: Wiley, 1995, ch. 8, pp. 200–248.
[2] J. Holtz, "Pulse-width modulation—a survey," *IEEE Trans. Ind. Electron.*, vol. 39, pp. 410–420, Oct. 1992.
[3] A. J. Trzydlanowski and S. Legowski, "Minimum-loss vector PWM strategy for three phase inverters," *IEEE Trans. Power Electron.*, vol. 9, pp. 26–34, Jan. 1994.
[4] A. J. Trzydlanowski and S. Legowski, "Applications of neural networks to the optimal control of three-phase voltage-controlled inverters," *IEEE Trans. Power Electron.*, vol. 9, pp. 397–397, July 1994.
[5] R. L. Kirlin, S. Kwok, A. J. Trzydlanowski, and S. Legowski, "Power spectra of a PWM inverter with randomized pulse position," *IEEE Trans. Power Electron.*, vol. 9, pp. 463–472, Sept. 1994.
[6] J. C. Candy and G. C. Temes, Eds., *Oversampling Delta-Sigma Data Converters—Theory, Design, and Simulation*. Piscataway, NJ: IEEE Press, 1991.
[7] S. Finco, F. H. Behrens, J. Guilherme, M. I. Castro Simas, and M. Lanca, "Pushing standard CMOS technologies into smart power conversion and amplification," *J. Circuits, Syst., Comp.*, vol. 5, no. 3, pp. 455–463, 1995.
[8] M. Carpita, M. Marchesoni, and L. Puglisi, "Power conditioning system using sliding mode control," in *IEEE Power Electronics Specialists Conf. (PESC) Rec.*, 1988, pp. 626–633.
[9] D. Casini, M. Marchesoni, and L. Puglisi, "Sliding mode multilevel control for improvement performances in power conditioning systems," *IEEE Trans. Power Electron.*, vol. 10, no. 4, pp. 453–463, July 1995.
[10] M. Carpita and M. Marchesoni, "Experimental study of a power conditioning system using sliding mode control," *IEEE Trans. Power Electron.*, vol. 11, no. 5, pp. 731–741, Sept. 1996.
[11] N. M. Abdel-Rahmin and J. E. Quaicoe, "Analysis and design of a multiple feedback loop control strategy for single phase voltage source UPS inverters," *IEEE Trans. Power Electron.*, vol. 11, pp. 532–541, July 1996.

Information Transmission using Chaotic Discrete-Time Filter

Adrian Leuciuc

***Abstract*—In this brief an adaptive approach for transmitting information hidden in a chaotic carrier is presented. The proposed method uses as a chaotic generator a discrete time nonlinear filter with a sawtooth nonlinearity induced by the two's complement overflow in digital filters. The synchronization at the receiving end is ensured by an adaptive slave system. Two different methods for hiding the information in the chaotic carrier are analyzed: direct chaos modulation and parameter modulation.**

***Index Terms*—Adaptive filters, chaos synchronization, information transmission using chaos.**

I. Introduction

Since Pecora and Carrol [1]–[3] published their results on chaos synchronization, the scientific community has manifested an increased interest in studying the many different aspects of using these principles in practical applications. A considerable effort has been made in applying synchronization of chaos in secure communications and data

Manuscript received June 19, 1998; revised November 11, 1998 and March 5, 1999. This paper was recommended by Associate Editor H. Kawakami.

The author is with the Department of Electrical and Computer Engineering, State University of New York at Stony Brook, on leave from the Technical University of Iaşi, Romania.

Publisher Item Identifier S 1057-7122(00)00731-5.

encryption [4]–[9]. At the beginning, the influence of the communication channel (frequency response and additive noise) and parameter mismatch between transmitter and receiver were not taken into account, or in a very small part. As practical communication schemes have been tried, the effect of these nonidealities, especially that of the noise on the channel, has proven to be destructive for the synchronization process. On the other hand, by increasing the robustness of the communication system, the confidentiality of the transmitted information can be lost. Efforts to improve the performances of the communication systems using chaos have been made. Several channel equalization methods were proposed in [10] and [11]; the differential chaos shift keying modulation reported in [12] has good noise performances; multiuser communication techniques were proposed in [13]–[15].

The results reported in this paper confirm the contrary requirements of a secure communication system using chaos and give an insight on how to design such a system in order to make a compromise between the desired confidentiality and robustness of the transmission. A particular discrete-time continuous-value chaotic system is considered. It consists of the all-pole IIR filter with a sawtooth nonlinearity in the feedback path shown in the left side of Fig. 1. Its simplicity and the possibility of easily extending it to a higher order make it a convenient chaotic generator. The statistical properties for the nonautonomous case and several methods for implementing it have been previously presented in the literature [9], [16]–[18]. In the previous analyses of this system, the nonlinearity was chosen to be the two's complement overflow one, as in digital filters, but as it will be pointed out in the next section, only the sawtooth shape is important for satisfying all its properties.

II. Error Performance Surface of the Adaptive Slave System

In this section we will consider the chaos synchronization setup depicted in Fig. 1. The nonlinearity is given by

$$f(x) = x - 2\,\mathrm{round}\left(\frac{x}{2}\right) \tag{1}$$

where $\mathrm{round}(x)$ stands for the nearest integer of x and the filter transfer function is an FIR type one

$$H(z) = \sum_{i=1}^{N} a_i z^{-i}. \tag{2}$$

It has been proven [18] that such a nonlinear system exhibits chaotic behavior if the linearized IIR filter is unstable. Furthermore, the output $y[k]$ has an N-dimensional uniform distribution if $a_N \in \mathbf{Z}, |a_N| > 1$ [9]. We must note that the exact two's complement overflow nonlinearity (1) is not a must, the system containing a general sawtooth shape nonlinear function exhibits similar properties. If the derivative of piecewise linear segments of $f(\cdot)$ has the value $K \neq 1$, this is equivalent with the introduction of a gain block K in front of the initial two's complement overflow nonlinear operator. This gain can be introduced in the transfer function of the feedback FIR filter, its effect being the altering of all filter coefficients by K. The functioning of the chaotic system is the same, including the N-dimensional uniform distribution of the output signal, if the linear subsystem remains unstable and $Ka_N \in \mathbf{Z}$, $|Ka_N| > 1$. Furthermore, if the lower and upper limits of $f(\cdot)$ are $[-b, b]$, $b \neq 1$, this is like a gain block with gain b is added at the output of the normalized nonlinearity and another one with gain $1/b$ at its input. Due to the feedback loop, the only effect of this modification is on the bounds of the output signal. Thus, the generated signal $y[k]$ remains chaotic, having the same statistical properties with respect to the new output limit values. In the following, without restricting the general case, the nonlinearity given by (1) will be considered. In the second part of this section we will see how the slave system structure from the right side of Fig. 1 has to be modified to ensure synchronization in the case of general sawtooth nonlinearity.

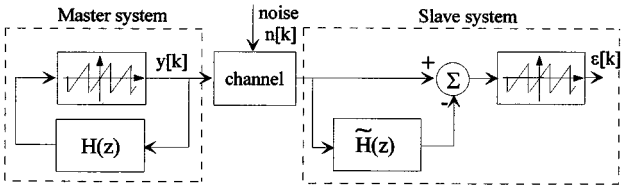

Fig. 1. The autonomous master–slave configuration for chaos synchronization.

The structure of the slave system of Fig. 1 is a feedforward one ensuring the synchronization in N clock periods if the nonlinearity and the filter tap weights are perfectly matched with the master system. If the FIR filter of the slave system has the parameters $\tilde{a}_i$, the synchronization error is

$$\varepsilon[k] = f\left(\sum_{i=1}^{N}(a_i - \tilde{a}_i)y[k-i]\right) = f\left(\sum_{i=1}^{N} x_i y[k-i]\right) \tag{3}$$

where $x_i = a_i - \tilde{a}_i$, $i = 1, \ldots, N$.

The performances of the adaptive algorithm used to eliminate the parameter mismatches can be derived from the shape of the error surface $\xi = E[\varepsilon^2[k]]$, where $E[\cdot]$ denotes the expectation. This error surface is also a measure for the level of confidentiality if we assume that when such a system is used for information transmission purposes, the statistics of the output signal $y[k]$ are independent of the information signal(s) statistics. In the following, we will consider that all the conditions ensuring the N-dimensional uniform distribution and ergodicity of the chaotic output signal $y[k]$ are met [9]. Analytical results were obtained for the first- and second-order systems, as well as for the Nth order one in the hypothesis that N is sufficiently large.

A. First-Order System

The mean square value of the synchronization error can be obtained in a simple manner and is given by

$$\xi(x_1) = \frac{x_1^2}{3} + \frac{2}{3}\frac{\mathrm{round}(\frac{x_1}{2})}{x}\left(1 - 3x_1^2 - 4\left(\mathrm{round}\left(\frac{x_1}{2}\right)\right)^2 + 6x_1\,\mathrm{round}\left(\frac{x_1}{2}\right)\right) \tag{4}$$

where $x_1 = a_1 - \tilde{a}_1$. In Fig. 2(a), the plots of the calculated (continuous line) and simulated (dotted line) mean square values of the synchronization error are shown. The simulations have been carried out using $a_1 = 4.5$ and the mean has been calculated over 10 000 samples. Even though the value of a_1 does not ensure the uniform distribution of $y[k]$, the two curves are very similar. The shape of the error performance surface presents multiple minima, and the convergence of a gradient-type adaptive algorithm to the correct value of a_1 is ensured for a maximum mismatch $|x_1| = |a_1 - \tilde{a}_1| = 1.3473$. For integer

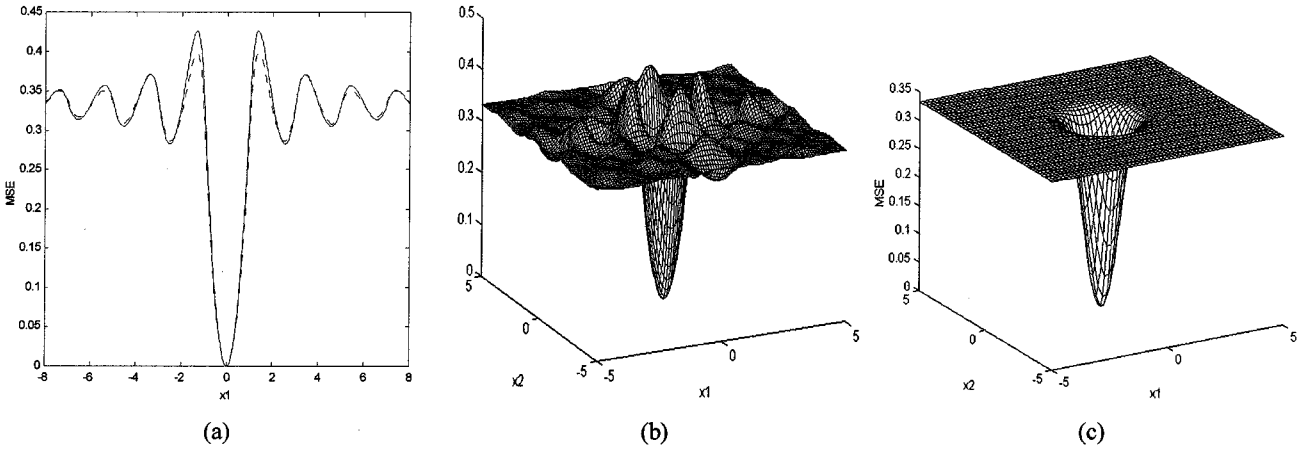

Fig. 2. Error performance surface for (a) first-order system: computed (continuous line) and simulated (dotted line); (b) second-order system; and (c) high-order systems (shown for $\boldsymbol{N = 2}$).

values of x_1, $\xi(x_1) = \frac{1}{3}$, the variance of a uniform distributed signal in $[-1, 1]$. The same value is obtained for $x_1 \to \infty$ and we will call it the saturation level of the error performance surface.

B. Second-Order System

Starting from (3) and using the uniform distribution and independence properties of the random variables $y[k-1]$ and $y[k-2]$, the following expression of the MSE was obtained:

$$\xi = \frac{4M_1}{3(p+q)} + \frac{1}{6(p^2-q^2)}\Big[(p-2M_2)^4 - (q-2M_1)^4 + 8p(M_2-M_1) - 8\Big(M_2^2 - M_1^2\Big)\Big] \tag{5}$$

where $p = |x_1| + |x_2|$, $q = ||x_1| - |x_2||$, $M_1 = \text{round}(\frac{q}{2})$, $M_2 = \text{round}(\frac{p}{2})$, $x_i = a_i - \tilde{a}_i$, $i = 1, 2$. This surface is depicted in Fig. 2(b), a similar shape being obtained by simulation. For any integer pairs (x_1, x_2) and for $x_1 \to \infty$ and/or $x_2 \to \infty$, $\xi(x_1, x_2) = \frac{1}{3}$, the saturation level.

C. Nth Order System

The calculus of the performance surface for a system of order $N > 2$ is laborious. Nevertheless, if the order N is large enough, the probability density function of the random variable $\sum_{i=1}^{N}(a_i - \tilde{a}_i)y[k-i]$ tends to a normal distribution function with variance $\sigma^2 = \frac{1}{3}(x_1^2 + \cdots + x_N^2)$, $x_i = a_i - \tilde{a}_i$, $i = 1, \cdots, N$ [21]. Thus, after some mathematical manipulations, the mean square error is given by

$$\xi = \sigma^2 + \frac{4}{\sqrt{2\pi}}\left[\frac{1}{\sigma}\sum_{k=-\infty}^{k=\infty}\left(k^2\int_{2k-1}^{2k+1} e^{-\frac{z^2}{2\sigma^2}}\,dz - e^{-\frac{(2k+1)^2}{2\sigma^2}}\right)\right]. \tag{6}$$

An intuitive representation of how this hypersurface in the $N+1$ dimensional space looks like can be obtained if we make $N = 2$, that is, $\sigma^2 = \frac{1}{3}(x_1^2 + x_2^2)$ in (6) and plot the result in Fig. 2(c). The gradient approximately equals zero everywhere, with the exception of a small neighborhood around the minimum. This makes impossible the convergence of a gradient-type adaptive algorithm if the initial values of the slave coefficients are not close enough to the correct values. The same value is obtained for the saturation level

$$\lim_{\sigma^2 \to \infty} \xi = \frac{1}{3}. \tag{7}$$

If the influence of the additive channel noise $n[k]$ is taken into account, the synchronization error becomes

$$\varepsilon[k] = f\left(n[k] - \sum_{i=1}^{N}(a_i + x_i)n[k-i] + \sum_{i=1}^{N} x_i y[k-i]\right). \tag{8}$$

For perfectly matched master and slave systems, $x_i = 0$, $i = 1, \cdots, N$, the synchronization error depends only on the channel noise. The influence of the noise on the synchronization is higher if the transmitter filter coefficients a_i have larger magnitudes. Thus, given a certain SNR on the channel, the synchronization error can be minimized if the sum $S = \sum_{i=1}^{N} a_i^2$ is minimum, keeping in mind that we must fulfill the conditions ensuring the chaotic behavior of the master system and its statistical properties.

The effect of the channel noise over the shape of the error performance surface can be viewed from the plots of Fig. 3. In Fig. 3(a) the simulated error performances surfaces in the one-dimensional (1-D) case are depicted for a channel SNR =10 dB (Gaussian white noise) and different values of a_1. These plots slightly change if the channel noise has distribution other than normal, but qualitatively the result is the same. Even the MSE does not null for $x_1 = 0$; the correct value of the transmitter coefficient can be still retrieved at the receiver using a gradient-type adaptive algorithm if we start from an initial value close enough to the exact one and the minimum has not reached a value close to the saturation level. The mean square value of the error for different values of SNR and S in the three dimensional (3-D) matched parameters case is plotted in Fig. 3(b). One can see that using a master filter with coefficients having $S = 20$, the same MSE is obtained as in the case $S = 6$ for a 5-dB higher SNR.

From the point of view of transmission secrecy, the presence of the noise on the channel, within reasonable limits, can be viewed as a positive fact as well. Indeed, if an unauthorized receiver tries to identify

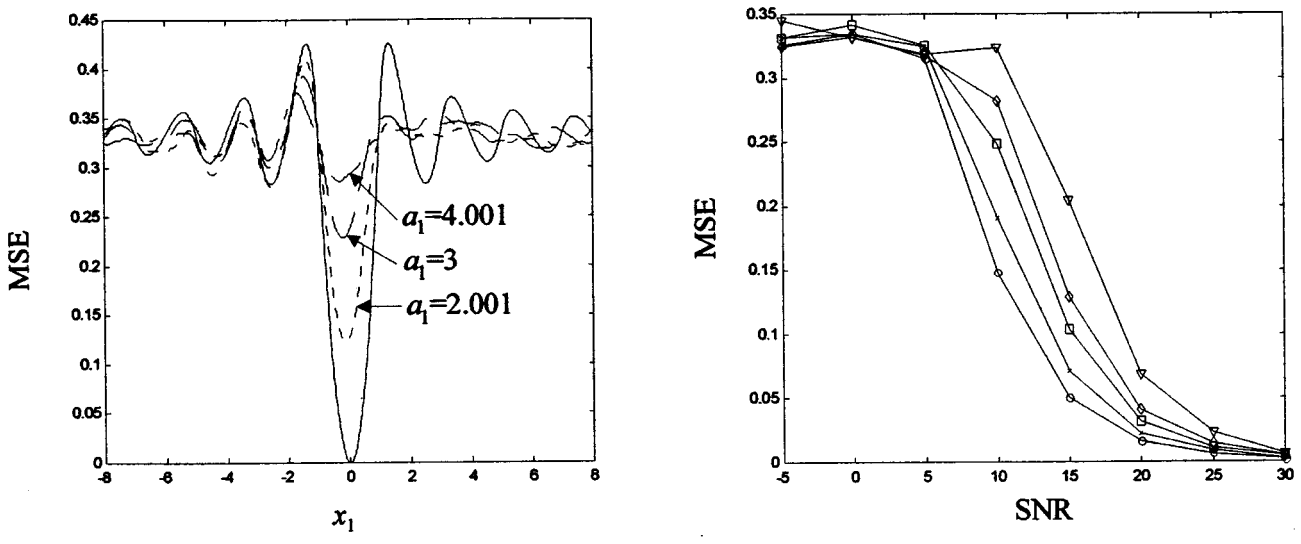

Fig. 3. Effect of channel noise on the synchronization error. (a) Error performance surface for a first order system (SNR = 0 dB-continuous line, SNR = 10 dB-dotted lines). Noninteger even values were considered for a_1 to avoid the nulling of $y[k]$ due to the finite binary representation of numbers in computer simulations. (b) MSE for a third-order synchronization system with matched parameters: ○—$a_1 = a_2 = 0.1, a_3 = 2$ $(S = 4.02)$; ×—$a_1 = 1, a_2 = -1.1, a_3 = 2$ $(S = 6.01)$; □—$a_1 = 2, a_2 = -1.1, a_3 = 2$ $(S = 9.01)$; ◊—$a_1 = 2.1, a_2 = -2, a_3 = 2$ $(S = 12.01)$; ∇—$a_1 = 3.2, a_2 = 2.4, a_3 = 2$ $(S = 20)$.

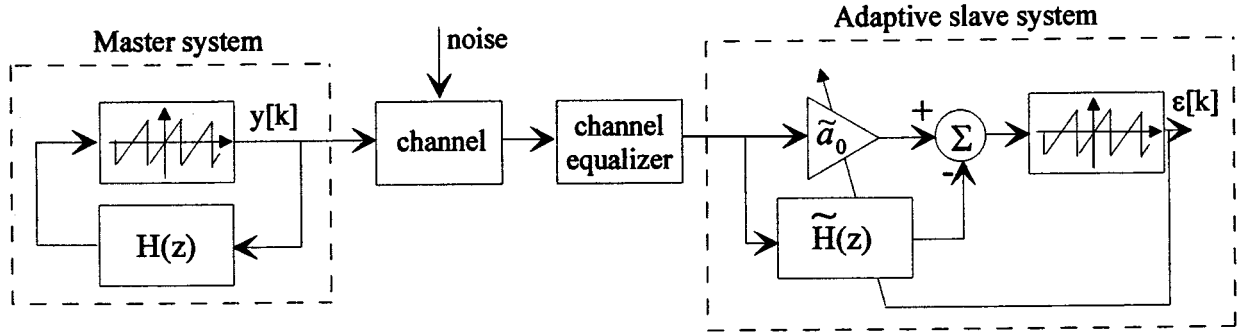

Fig. 4. The autonomous master–adaptive slave configuration for chaos synchronization.

the chaotic master system when noise is not present, he will always know if the identification is achieved or not from the value of the MSE. Different combinations of the parameters can be tried until the correct values are obtained. In the case of a noisy channel, the value of the minimum of the error surface is different to zero, comparable to other local minima, and the task of the intruder is more difficult.

Following all the conclusions from above, the general synchronization scheme using an adaptive slave system is depicted in Fig. 4. The difference, compared to the scheme in Fig. 1, is the supplementary gain block $\tilde{a}_0$ in the slave structure. This adaptive gain block is used to compensate for the different slope of the transmitter nonlinearity when this has a general sawtooth shape, as discussed in the beginning of the section. Thus, if the transmitter nonlinearity is characterized by a slope K and is bounded within the interval $[-b, b]$, it can be easily verified that the synchronization is achieved if

$$\begin{aligned} &K\tilde{a}_0 a_i = \tilde{a}_i, \qquad i = 1, \ldots, N \\ &\frac{\tilde{K}\tilde{a}_0 b}{\tilde{b}} \in \mathbf{Z}. \end{aligned} \tag{9}$$

Even in the case of identical nonlinear characteristics at both ends of the synchronization configuration ($K = \tilde{K},\ b = \tilde{b}$), there is a infinite, countable set of receiver parameters for which the synchronization is achieved: $\{\tilde{a}_0 = m/K,\ \tilde{a}_i = ma_i\}, m \in \mathbf{Z} - \{0\},\ i = 1, \ldots, N$. Finally, as it can be seen from Fig. 4, the complete receiver scheme contains an equalizer to compensate the frequency response of the transmission channel, but this aspect will not be addressed here.

III. Direct Chaos Modulation Approach

If we want to use the chaos synchronization configuration in Fig. 4 for confidential information transmission purposes, there are two possibilities for hiding the signal to be transmitted in the chaotic carrier: the direct chaos modulation approach and the parameter modulation approach. In this section, the performances of the former is analyzed. The modulating signal $m[k]$ is added at the input of chaotic generator and the synchronizing slave remains unchanged. The output of the slave system, when ideal channel and perfectly matched parameters are considered, is equal to the modulating signal $m[k]$ if $|m[k]| < 1$ [9]. If the parameter mismatch is taken into account, the output of the receiver is

$$\varepsilon[k] = f\left(m[k] + \sum_{i=1}^{N} x_i y[k-i]\right) \tag{10}$$

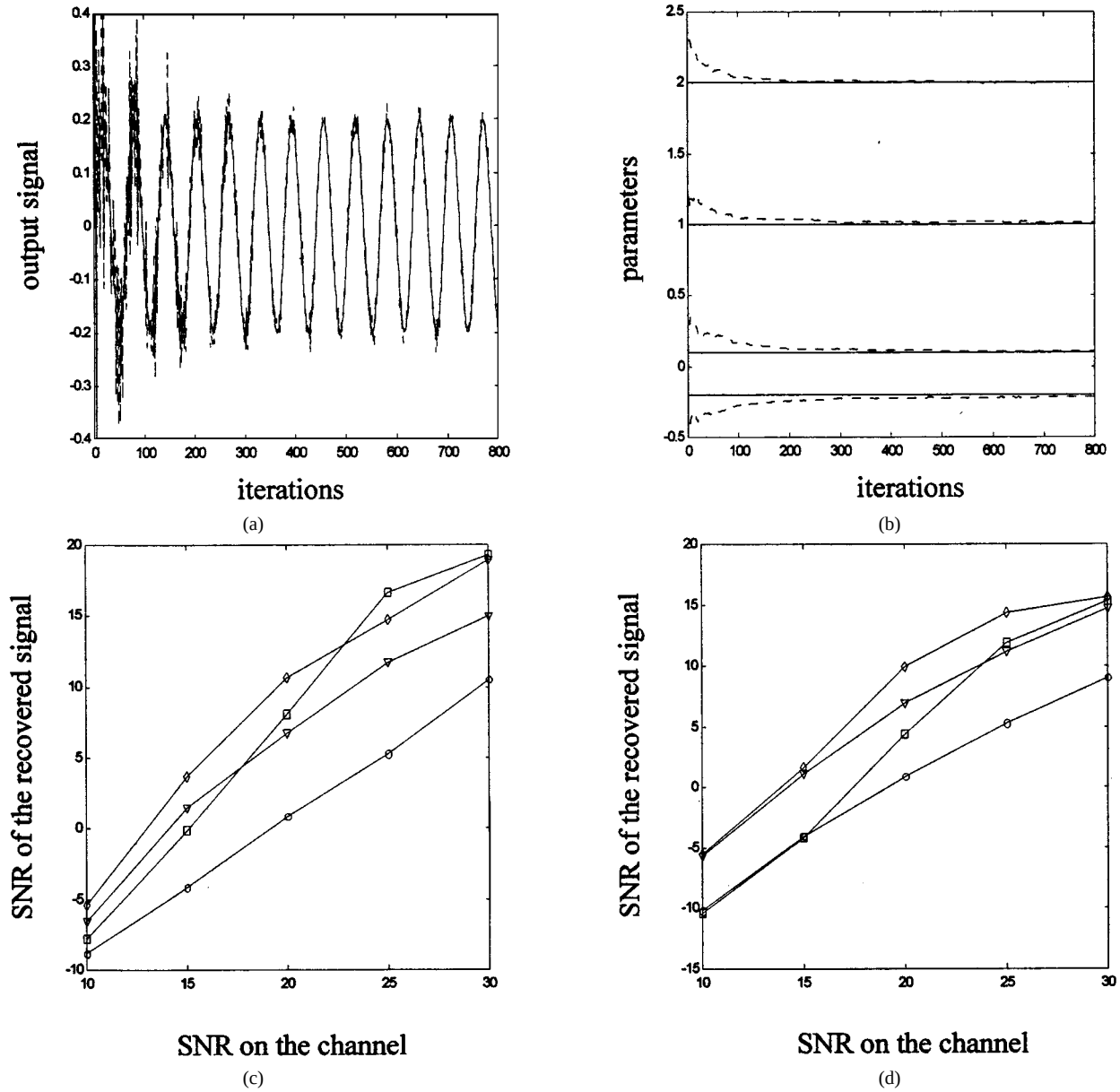

Fig. 5. Simulation results for direct chaos modulation. (a) Recovered signal for the open loop receiver with matched parameters (continuous line) and closed adaptive loop (dotted line). (b) Parameter convergence of the adaptive receiver $(\boldsymbol{a}_1 = 0.1, \boldsymbol{a}_2 = -0.2, \boldsymbol{a}_3 = 2, \tilde{\boldsymbol{a}}_0[0] = 1.2, \tilde{\boldsymbol{a}}_1[0] = 0.3, \tilde{\boldsymbol{a}}_2[0] = -0.4, \tilde{\boldsymbol{a}}_3[0] = 2.3)$. (c) SNR of the recovered signal vs. SNR on the channel for the open-loop, matched parameters receiver. (d) SNR of the recovered signal versus SNR on the channel for the closed-loop adaptive receiver. (○—$\boldsymbol{A} = 0.2$; ∇—$\boldsymbol{A} = 0.4$; ◊—$\boldsymbol{A} = 0.6$; □—$\boldsymbol{A} = 0.8$.)

where, for simplicity, the nonlinearity $f(\cdot)$ is given by (1) and considered throughout the rest of this paper. Equation (10) is similar to (8), the modulating signal $m[k]$ replacing the noise terms. Thus, taking into account that $m[k]$ and the chaotic carrier $y[k]$ are uncorrelated, the adaptive algorithm used at the receiving end will converge toward the correct values of the parameters if the variance of $m[k]$ is smaller than the saturation level. Because $|m[k]| < 1$, after the adaptation process converges $\varepsilon[k] = m[k]$. Since the effect of the modulating signal is similar to that of the additive noise channel, the closer the variance of $m[k]$ to the saturation level, the higher the level of secrecy of such a communication system is. In this case the authorized receiving part has to know exactly the parameter values used at the transmitter. The identification process is not possible anymore, even if the initial values of the receiver parameters are very close to the transmitter ones. In Fig. 5 several simulation results for this setup are given, the modulating signal being a sinusoid and using a third-order system with RLS adaptive algorithm. The results obtained in the case of adaptive receiver are compared to the ones corresponding to an open-loop receiver with matched parameters.

Similar results have recently been reported in [23] where the identification of the chaotic transmitter is determined in a noiseless environment by evaluating the variance of the error signal σ_e^2 and then searching for the maximum of $|\sigma_e^2 - \frac{1}{3}|$. This method can identify the parameters of the transmitter even for modulating signals with variance larger than the saturation level, performance which cannot be achieved with our approach without *a priori* information about $m[k]$. However, the method proposed in [23] is timewise and computationally more expensive than the adaptive approach presented herein.

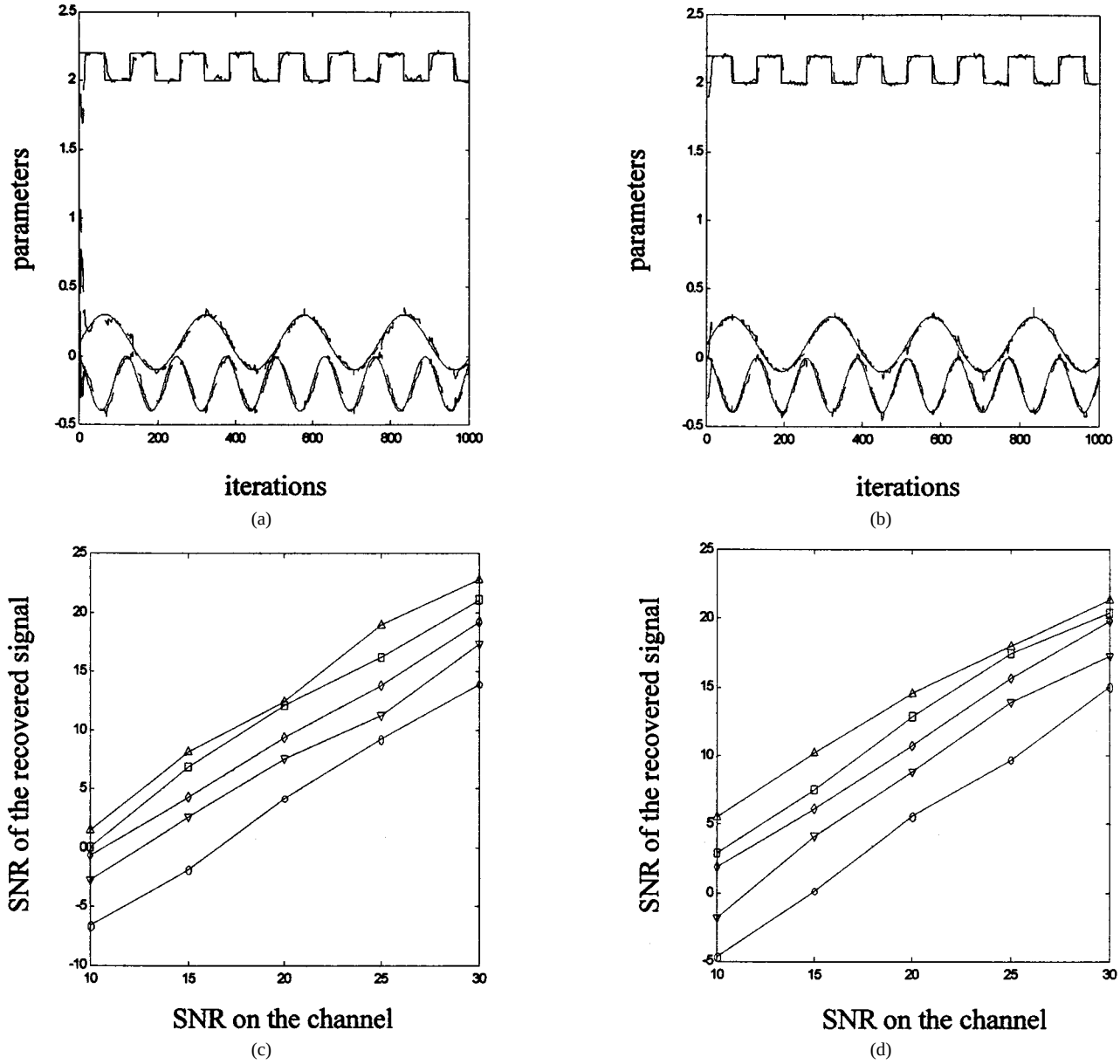

Fig. 6. Simulation results for parameter modulation. (a) Recovered signals—NLMS adaptive filter. (b) Recovered signals—Kalman filter. (c) SNR of the recovered signal versus SNR on the channel—NLMS adaptive filter. (d) SNR of the recovered signal versus SNR on the channel—Kalman filter. ($\bigcirc$—$\boldsymbol{A} = 0.1$; ∇—$\boldsymbol{A} = 0.15$; $\Diamond$—$\boldsymbol{A} = 0.2$; $\square$—$\boldsymbol{A} = 0.25$; $\triangle$—$\boldsymbol{A} = 0.3$.)

IV. Parameter Modulation Approach

Another way to transmit information using chaos is the parameter modulation technique [13], [24], [25]. One can use several information signals to modulate the filter coefficients of the master system in Fig. 4. Using an adaptive receiver and appropriate adaptive algorithms with good tracking performances, the information can be recovered if the amplitude and bandwidth of the modulating signals are not too large. The parameter modulation approach has the main advantage of being less sensitive to noise compared to direct chaos modulation approach. At the same time it offers the possibility of multiple parameter modulation, resulting in simultaneous multiple access of a single communication channel. However, the bandwidth of the modulating signal(s) is reduced due to the low-pass filtering effect of adaptive algorithms. For example, in the case of LMS algorithm, the taps of the adaptive FIR filter are updated using the iteration

$$\tilde{a}_i[k+1] = \tilde{a}_i[k] + \mu\varepsilon[k]y[k-i] \tag{11}$$

where μ is the adaptation parameter. The convergence in the mean square is ensured if $\mu < \frac{2}{\mathrm{trace}(R)}$ where R is the $N \times N$ autocorrelation matrix of $y[k]$ [26]. Assuming the conditions for the N-dimensional uniform distribution of $y[k]$ satisfied, all the eigenvalues of R are equal to σ_y^2 and $\mathrm{trace}(R) = N\sigma_y^2 = \frac{N}{3}$. The LMS algorithm is derived from the steepest descent method for finding the minimum of the error surface and, consequently, the time constant associated to the transient of filter coefficients, when all the eigenvalues of R are equal, is given by $\tau \approx \frac{1}{\mu\sigma_y^2}$, being proportional with the filter order N. It

follows that we can approximate the -3 dB bandwidth of the adaptive algorithm by $f_{3\,\mathrm{dB}} = \mu\sigma_y^2 f_{\mathrm{clk}}$.

Numerous computer simulations have been carried out using different adaptive algorithms. In Fig. 6, some representative results are presented. NLMS and Kalman filters were considered, the RLS algorithm being known for its poor tracking performances [26]. Comparing the results in Fig. 6 to the results in Fig. 5, one can see that the noise performances of the parameter modulation approach are better than those of the both open and closed loop structures in the case of direct modulation technique.

V. Conclusion

In this paper, the possibilities of using the chaotic discrete-time filter with sawtooth nonlinearity in confidential information transmission are analyzed. The effects of parameter mismatch and channel noise on the chaos synchronization are considered. Analytic expressions for the error performance surface of the adaptive synchronizing inverse system were derived, showing that the chaotic master system can be identified if the parameter mismatch is relatively small.

Two different approaches for using the analyzed configuration for secure information transmission using chaos were compared: direct chaos modulation and parameter modulation. This comparison revealed that parameter modulation technique has better noise performances, simultaneously offering the possibility of transmitting multiple signals hidden within the same chaotic carrier. Nevertheless, the low-pass filtering effect of adaptive algorithms decrease the bandwidth of the transmitted signals. It was shown that the channel noise, if moderate, besides its well-known negative effect on the signal recovery, can improve the confidentiality of the transmission by lowering the identification chances of an unauthorized receiver. As it has been pointed out in previous publications as well, the performances of communication systems using chaos are poorer compared to classical methods. However, the parameter modulation method can be used with good performances in digital data encryption, the results of this approach to be published elsewhere.

References

[1] L. M. Pecora and T. L. Carroll, "Synchronization in chaotic systems," *Phys. Rev. Lett.*, vol. 64, no. 8, pp. 821–824, Feb. 1990.

[2] T. L. Carroll and L. M. Pecora, "Synchronizing chaotic circuits," *IEEE Trans. Circuits Syst.*, vol. 38, pp. 453–456, Apr. 1991.

[3] L. M. Pecora and T. L. Carroll, "Driving systems with chaotic signals," *Phys. Rev. A*, vol. 44, no. 4, pp. 2374–2383, Aug. 1991.

[4] M. Hasler, "Engineering chaos for encryption and broadband communication," *Phil. Trans. R. Soc. London*, vol. 352, pp. 1–12, 1995.

[5] K. M. Cuomo and A. V. Oppenheim, "Circuit implementation of synchronized chaos with applications to communications," *Phys. Rev. Lett.*, vol. 71, no. 1, pp. 65–68, 1993.

[6] C. W. Wu and L. O. Chua, "A simple way to synchronize chaotic systems with applications to secure communication systems," *Int. J. Bifurcation Chaos*, vol. 3, no. 6, pp. 1619–1627, June 1993.

[7] U. Parlitz, L. Kocarev, T. Stojanovski, and H. Preckel, "Encoding messages using chaotic synchronization," *Phys. Rev. E*, vol. 53, no. 5, pp. 4351–4361, 1996.

[8] T. Yang, C. W. Wu, and L. O. Chua, "Cryptography based on chaotic systems," *IEEE Trans. Circuits Syst. I*, vol. 44, pp. 469–472, May 1997.

[9] M. Gotz, K. Kelber, and W. Schwarz, "Discrete-time chaotic encryption systems—Part I: Statistical design approach," *IEEE Trans. Circuits Syst. I*, vol. 44, pp. 963–970, Oct. 1997.

[10] F. Böhme and M. P. Kennedy, "Compensation of linear stationary channel influence in chaos communication," in *Proc. NDES'96*, Sevilla, Spain, June 27–28, 1996, pp. 93–98.

[11] H. Leung, "System identification using chaos with application to equalization of a chaotic modulation system," *IEEE Trans. Circuits Syst. I*, vol. 45, pp. 314–320, Mar. 1998.

[12] G. Kolumbán, B. Vizvári, W. Schwarz, and A. Abel, "Differential chaos shift keying: A robust coding for chaotic communication," in *Proc. NDES'96*, Sevilla, Spain, June 27–28, 1996, pp. 87–92.

[13] U. Parlitz and L. Kocarev, "Multichannel communication using autosynchronization," *Int. J. Bifurcation Chaos*, vol. 6, no. 3, pp. 581–588, Mar. 1996.

[14] V. Miljanovic, K. M. Syed, and M. E. Zaghloul, "Chaotic communications by CDMA techniques," in *Proc. NDES'96*, Sevilla, Spain, June 27–28, 1996, pp. 155–160.

[15] D. J. Sobiski and J. S. Thorp, "PDMA-1: Chaotic communication via the extended Kalman filter," *IEEE Trans. Circuits Syst. I*, vol. 45, pp. 194–197, Feb. 1998.

[16] K. Kutzer, W. Schwarz, and A. C. Davies, "Chaotic signals generated by digital filter overflow," in *Proc. ISCAS'94*, vol. 6, 1994, pp. 17–20.

[17] M. Gotz, K. Kelber, and W. Schwarz, "Discrete-time chaotic coders for information encryption. Part 1: Statistical approach to structural design," in *Proc. NDES'96*, Sevilla, Spain, June 27–28, 1996, pp. 15–20.

[18] K. Kelber, T. Falk, M. Gotz, W. Schwarz, and T. Kilias, "Discrete-time chaotic coders for information encryption. Part 2: Continuous- and discrete value realization," in *Proc. NDES'96*, Sevilla, Spain, June 27–28, 1996, pp. 21–25.

[19] H. Dedieu and M. J. Ogorzalek, "Identifiability and identification of chaotic systems based on adaptive synchronization," *IEEE Trans. Circuits Syst. I*, vol. 44, pp. 948–962, Oct. 1997.

[20] U. Feldmann, M. Hasler, and W. Schwarz, "Communication by chaotic signals: The inverse system approach," *Int. J. Circuits Theory Appl.*, vol. 24, no. 4, pp. 551–580, 1996.

[21] A. Papoulis, *Probability, Random Variables, and Stochastic Processes*. New York, NY: McGraw-Hill, 1991.

[22] A. Leuciuc and V. Grigoraş, "Simulation results on discrete-time filter adaptive chaos synchronization," in *Proc. ECCTD'97*, vol. 3, Budapest, Hungary, 1997, pp. 1231–1236.

[23] F. Dachselt, K. Kelber, and W. Schwarz, "Discrete-time chaotic encryption systems—Part III: Cryptographical analysis," *IEEE Trans. Circuits Syst. I*, vol. 45, pp. 983–988, Sept. 1998.

[24] N. J. Corron and D. W. Hahs, "A new approach to communications using chaotic signals," *IEEE Trans. Circuits Syst. I*, vol. 44, pp. 373–382, May 1997.

[25] T. Yang and L. O. Chua, "Secure communication via chaotic parameter modulation," *IEEE Trans. Circuits Syst. I*, vol. 43, pp. 817–819, Sept. 1996.

[26] S. Haykin, *Adaptive Filter Theory*. Englewood Cliffs, NJ: Prentice Hall, 1991.